ENVIRONMENTAL RESEARCH
LETTERS

ACCEPTED MANUSCRIPT • OPEN ACCESS

Comment on “Linkage of El Niño-Southern Oscillation to astronomic forcing”

To cite this article before publication: Richard Ray *et al* 2025 *Environ. Res. Lett.* in press https://doi.org/10.1088/1748-9326/add1f2

Comment on "Linkage of El Niño-Southern Oscillation to astronomic forcing"

Richard Ray[1] **& Carl Wunsch**[2]
[1] Geodesy & Geophysics Laboratory, NASA Goddard Space Flight Center, Greenbelt, USA
[2] Harvard University, Cambridge, USA
E-mail: `richard.ray@nasa.gov`

15 February 2025

1. Introduction

Valle-Levinson (2024) (hereinafter, VL24) reports that the El Niño–Southern Oscillation (ENSO), one of the most important climate phenomena in the Earth system, may be "linked" to certain orbital motions of the moon as well as to the sun's 11-year and 22-year solar cycles. His evidence is based primarily on successful curve-fitting, with little physical justification other than the obvious ones: that solar cycles modulate insolation and that lunar motions induce tides, which can impact ocean mixing. An explicit physical connection to ENSO was not attempted. Nonetheless, VL24 concludes that "the linkage between astronomic forcing and ENSO should be further explored with Earth system climate models."

The VL24 cycle-fitting was subsequently extended by Valle-Levinson & Pattiaratchi (2024) (hereinafter VLP24) to other climate indices, such as the Pacific Decadal Oscillation, the Indian Ocean Dipole, etc. In an earlier report, Valle-Levinson et al. (2021) applied similar cycle-fitting, with similar interpretations, to annual mean sea levels at Venice and Trieste, concluding that the interannual sea-level variability there "can be mostly explained with astronomic forcing," and that this allows sea-level variations to be projected into the rest of the 21st century.

One may readily grant that ENSO is so intertwined with many complex and subtle atmospheric and oceanic interactions that it is conceivable that some lunar forcings, as well as the solar cycle, could have some influence on it. However, the conclusion of VL24 is that the interannual variability of ENSO is largely dominated by the astronomy, in the sense that a linear regression against astronomical frequencies provides not only a good statistical fit, but one that can be projected into the future. Those strong conclusions are without foundation.

The history of science is filled with attempts to explain a huge variety of phenomena by claiming them to be the result of periodic forcing. One illuminating example is the review by Pittock (1978) who clearly describes the pitfalls of explaining a multitude of phenomena by the solar cycle.

This comment comprises two main sections. One addresses the technical details of the VL24 simulations that purport to show that the frequency-fitting, when applied to the ENSO time series, results in a satisfactorily high goodness-of-fit (quantified by his R^2 statistic) that cannot be similarly obtained with random time series. This is taken to substantiate the statistical significance of the cycle-fitting. The second section addresses the more fundamental issue of the physical rationale, or lack thereof, of ENSO being explainable by a few dozen astronomical-based cycles, and whether these purported cycles exist, or even could exist, in the climate system.

In brief summary, the following two sections show there is neither statistical nor physical evidence for a connection between ENSO and these multiple astronomical cycles.

2. Simulation experiments

The idea behind the simulation experiments of VL24 is a good one. We should like to know whether any random time series could be fitted as well as the ENSO time series is, using the given astronomical frequencies. The VL24 results show that random time series cannot be so fit. Our objections address two critical issues: (1) what is meant by "random" and whether that is appropriate to the problem at hand, and (2) which astronomical frequencies are employed.

Here we repeat the VL24 simulations, but in a manner that addresses our objections. As in VL24, we use the nino3.4 index, spanning years 1870–2023.

2.1. Characteristics of random time series

By random time series, VL24 meant a pure white-noise process, produced with a uniform random number generator. ENSO is certainly not a white-noise process, and we should not expect a time series based on such a process to be explainable by any set of astronomical frequencies, even after the series is low-pass filtered. It is more appropriate to use random time series that are in some sense ENSO-like, based on some physical or statistical characteristics of the real time series. Ambaum (2010) nicely summarizes the problem as follows: We require

> . . . synthetic time series with similar properties. . . to the original time series but [which] are unrelated by construction. Note that this is by no means a trivial exercise: to produce the synthetic data, we need to use a model that is as faithful as possible to the original model, except for the fact that, by construction, the synthetic series is based on a model in which the hypothesized relationship is explicitly switched off. (Ambaum, 2010).

In the case at hand, the hypothesized relationship is that the ENSO index is mostly the sum of a set of harmonics with certain (astronomical) frequencies.

There are several alternative methods that are typically used in these kinds of time series simulations (e.g., Davison & Hinkley, 1997). Here, to simulate ENSO in a manner more physically realistic than a uniform random number generator, we employ the widely-used technique of "phase scrambling" (Davison & Hinkley, 1997), in which a periodogram—roughly similar in shape to the real ENSO periodogram—is used, but each frequency component of the underlying Fourier series is assigned a random phase in the interval $[0, 2\pi]$. Timmer & König (1995) point out that the method should also invoke amplitude

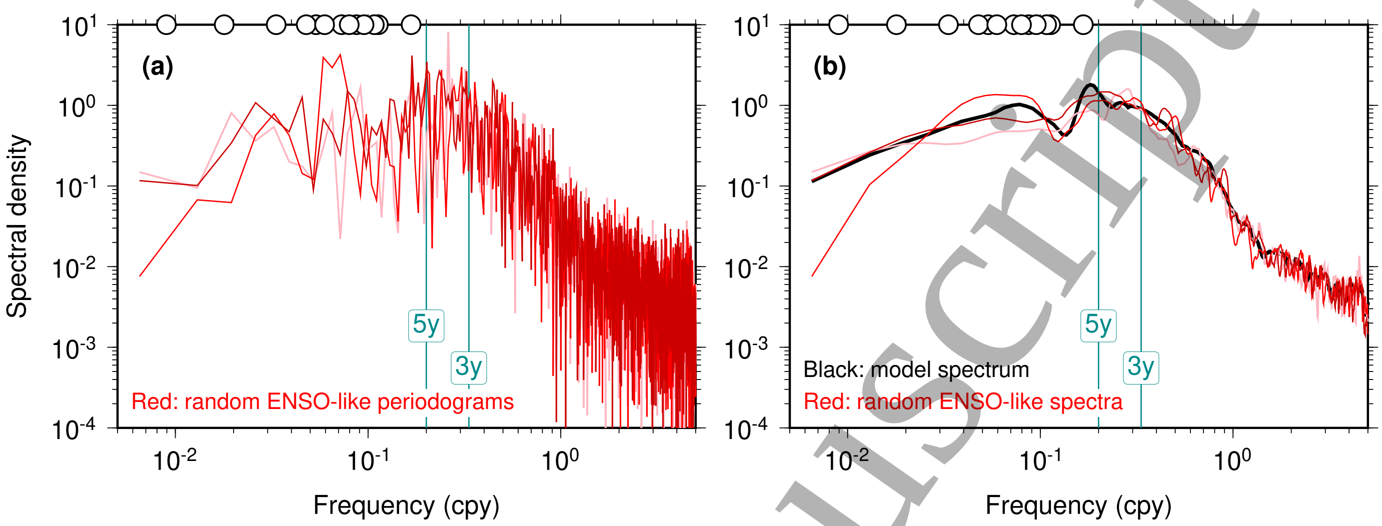

Figure 1. (a) Periodograms of three random realizations of ENSO-like time series, in slightly different shades of red. (b) Their corresponding spectra. In black is the spectral estimate of the real ENSO time series, smoothed to remove any possible spectral peaks corresponding to VL24's astronomical frequencies. Blue vertical lines are the low-pass filter cutoffs used by VL24. Circles across top axes mark the 13 frequencies used by VL24 to fit sinusoids to the ENSO time series. Below the 5-y filter cutoff, the circles are seen to cover most Fourier frequencies.

randomization, and that is clearly necessary here since phase randomization alone is unlikely to affect subsequent cycle-fitting. We thus scale the spectral density at each frequency by a χ_2^2 random variable, consistent with the expected variance in a periodogram (Percival & Walden, 1993). (The original Timmer–König paper discusses power-law noise, but their technique is applicable to any type of spectrum). Finally, in accordance with Ambaum's point quoted above, we ensure that VL24's hypothetical astronomical cycles are "switched off" in the synthetic series by applying a heavy smoother to the ENSO periodogram. That ensures the model spectrum, which is used to generate all subsequent synthetic time series, has no possible astronomical cycles in it, or at least none above background.

An example of three random realizations is shown in the spectral domain in Figure 1a. Their corresponding spectra (highly smoothed periodograms) are in Figure 1b. With phase scrambling, the three different periodograms are used to generate random time series which are ENSO-like, in the sense their smoothed spectra more or less agree with the real ENSO spectrum, as in panel (b). The spectra of these structured random data are obviously more representative of ENSO reality than is a flat, white spectrum.

One example of a random ENSO-like time series, generated from one of the periodograms of Figure 1a, is shown in Figure 2, at its original monthly sampling and also after application of the Lanczos-type 3-year filter that VL24 employed. One sees the similarity in character of the real and the random time series, even though the latter does not correspond to reality in terms of times or magnitudes of ENSO anomalies.

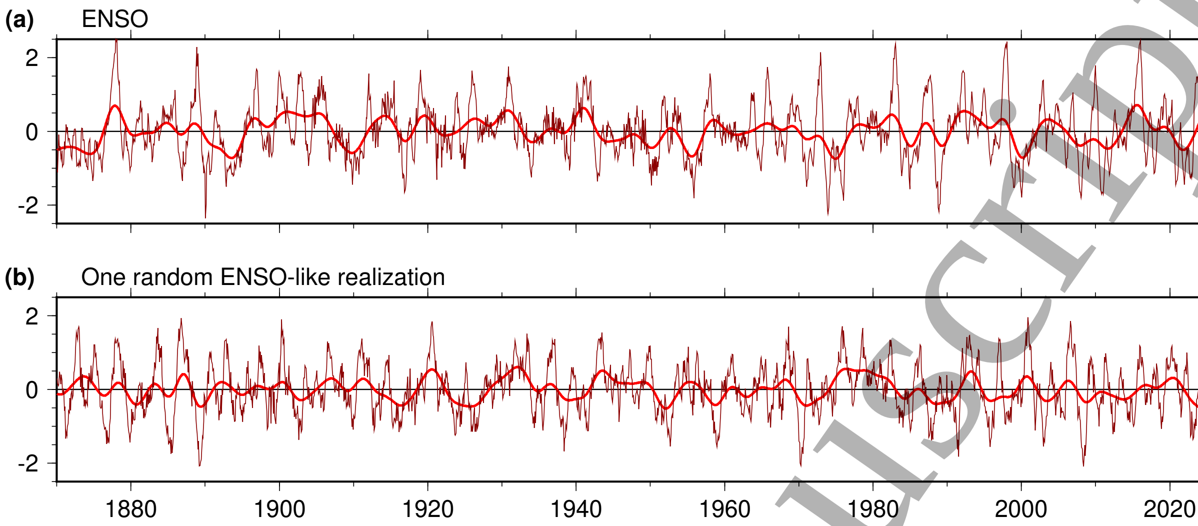

Figure 2. (a) ENSO (nino34) index time series in thin line (deseasoned); 3-year low-pass filtered series in heavy red line. (b) One random realization of a ENSO-like time series, based on phase scrambling of the ENSO smoothed spectrum, with Fourier amplitude randomization following Timmer & König (1995), in thin line; 3-y filtered series in heavy red line.

2.2. Choice of astronomical frequencies

The second problem with the VL24 simulations is that the suite of 13 astronomical frequencies have been selectively chosen (or "cherry picked") to perform well when fitting to the real ENSO time series. This is evident in part by the choice of frequencies in his Table 1. For example, we see (as expected) the period of the lunar node, $T_N = 18.6$ y, but also certain multiples of it: $(T_N/2, 3T_N, 6T_N)$. Why not $2T_N, 4T_N, 5T_N$ or $T_N/4$? The selective frequency-picking is made explicit by VLP24 when they fit to ENSO as well as to 6 other climate indexes, and their Table 1 does include other multiples of T_N: specifically multiples of 2, 3, 4, and 6 (why not 5?). VLP24 actually examine two different sets (of 18 frequencies), based on whether the solar cycle is defined by periods 10.5 and 11.5 y, or by 10 and 11 y; that choice then generates five different "interaction" frequencies to select from. Some of these frequencies are applied by VLP24 to some climate time series and not to others. The choice is obviously dependent on "what works."

It is therefore appropriate to apply this same frequency-picking to the random ENSO time series being fitted. Thus, for each random time series, we examined the two sets of 18 frequencies of VLP24, and (following VL24) pick the 13 that results in the best fit.

2.3. Simulation results

We generated 10^5 random realizations of ENSO, filtered the series using either 3-y or 5-y low-pass filters, following VL24, and then selected 13 frequencies for fitting, as described above. The measure of goodness of fit uses the same R^2 statistic that VL24 used, essentially the fraction of explained variance, with higher R^2 representing a superior fit. The results are shown in the two histograms of Figure 3. The red vertical lines mark the R^2 obtained by fitting

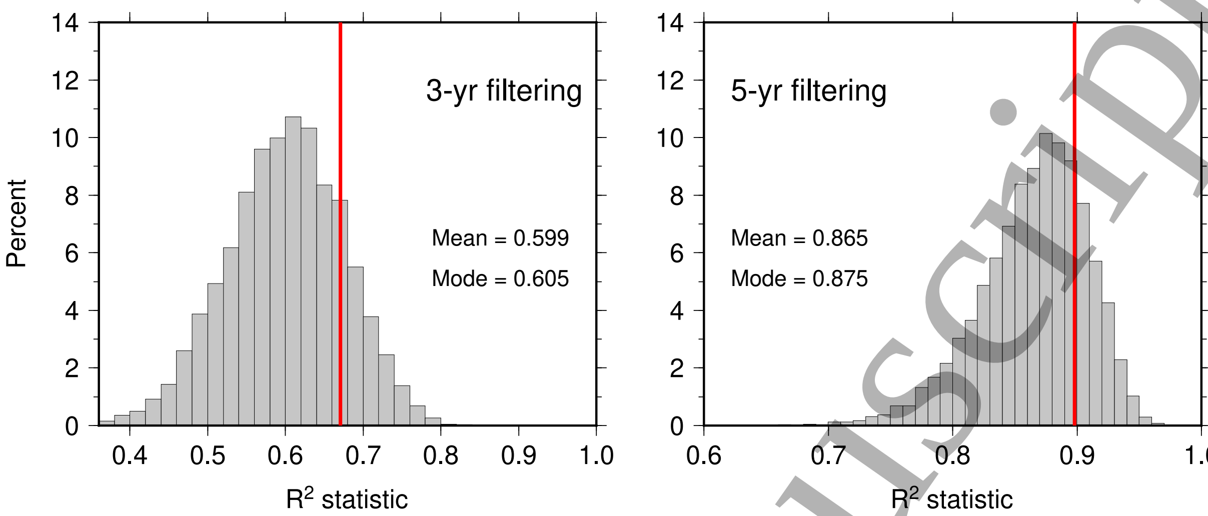

Figure 3. Histograms of the statistic R^2 (explained variance), obtained by fitting 13 sinusoids to 10^5 random time series, low-pass filtered at 3 y (left) or 5 y (right). Each random time series has an ENSO-like spectrum (as in Figure 1). Each fit used 13 frequencies selected from two possible sets of 18 frequencies, following Valle-Levinson & Pattiaratchi (2024). Red vertical lines mark the R^2 obtained from fitting the 13 frequencies of Valle-Levinson (2024) to the real ENSO time series. Both histograms should be compared with Figure 3 of Valle-Levinson (2024).

the real ENSO time series, which are 0.67 for the 3-y filtered series and 0.90 for the 5-y filtered series, in agreement with the numbers reported by VL24.

It is clear that a fairly large fraction of the random time series can be fit as well as, or better than, the real ENSO series can be fit. The number of values of R^2 exceeding the R^2 for the real ENSO data is 17% for the 3-y filtering and 23% for the 5-y filtering.

The exercise of fitting the ENSO series to astronomical cycles is therefore no more justified than fitting cycles to random data. Any interpretation of the fits is likely flawed and is unlikely to be revealing anything regarding the physical processes behind the ENSO phenomenon.

3. Physical rationale

Statistical considerations involving simulations and curve-fitting are important, but a more fundamental concern is the physical rationale underlying these astronomical cycles and whether they can be expected, on physical grounds, to appear in any climate time series, ENSO or not. The solar cycle(s) will not be addressed here; there is a large, often controversial, literature on the subject of solar cycles and climate (e.g., Pittock, 1978, 2009). At least for global temperatures, there appears to be a small effect which is mostly consistent with climate models (Amdur et al., 2021). ENSO is another matter, of course, but we will not comment. Below we concentrate on the supposed lunar cycles as well as various interaction frequencies.

3.1. Three lunar cycles?

VL24 and VLP24 employ three fundamental lunar cycles. From these, plus the solar cycles, they conjecture the presence of four, five, or six interaction frequencies, supposedly induced by "interference" between the fundamental cycles. The three fundamental lunar cycles are as follows:

Nodal cycle, period 18.6 y. This cycle is a physically realistic one and it does conceivably impact climate. The moon's nodal precession modulates all lunar tides, including major tides like M_2 and K_1. If these tides are involved in ocean mixing, and they surely are at some level, then a nodal cycle in climate could appear (e.g., Loder & Garrett, 1978; Osafune et al., 2020; Joshi et al., 2023). There is a large literature on the nodal cycle in climate, although much of it has been unconvincing, in part owing to the shortness of most climate time series. Stronger evidence is beginning to appear. Some of the best cases stem from the mixing effects of diurnal tides, whose nodal modulations are more pronounced than those of major semidiurnal tides (Osafune & Yasuda, 2013). Although the possibility of the nodal cycle appearing in certain kinds of climate series can be accepted, whether the cycle is actually present in ENSO is of course a separate question.

Perigee cycle, period 8.85 y. Any climate effect at a period around 8.85 y, associated with the precession of the lunar perigee, is unlikely. Unlike the nodal cycle, there is no similar 8.85-y modulation of any major tidal constituent that could be involved in ocean mixing.

There is a different possible mechanism, of a somewhat obscure nature, which involves harmonic beating between tides generated by second-degree versus third-degree terms[1] in the tidal potential. Every third-degree tidal constituent has a corresponding second-degree analogue, but separated in frequency by one cycle in 8.85 y. Probably the most important of these pairs is N_2 and its typically tiny third-degree counterpart, sometimes dubbed $^3N_2$ (the Doodson numbers are 245.655 and 245.555, respectively). Unlike standard nodal modulations, the two spectral lines in this case are unrelated by amplitude and any perceptible beating between them would be manifested only in special places where $^3N_2$ is unusually large. One such location is the Gulf of Maine where a clear 8.85-y modulation of N_2 becomes evident (Doodson, 1924; Ray & Talke, 2019). Of course, the Gulf of Maine tide is a special tidally resonant case; one cannot expect this mechanism to be at work in many other places of the ocean where N_2 and especially $^3N_2$ are much weaker (cf. Feng et al., 2015). Nor is N_2—generally 5 times weaker than M_2—considered a particularly important constituent for ocean mixing. A sensible climate effect from the 8.85-y lunar precession is thus doubtful.

VL24 (in Supplement) claims that "each location on Earth will exhibit their largest perigean spring tides at a cyclicity of 8.85 y." Valle-Levinson et al. (2021) make a similar assertion. If that statement were true, then the 8.85-y periodicity could possibly be important to climate. The statement, however, is incorrect. There is no physical reason why the orientation

[1] For differences between second-degree and very weak third-degree tides, see Godin (1988, pp. 238, 278).

of the moon's ellipse should perturb spring tides at 8.85 y, and we know of no case from any tide gauge that displays such a periodicity in perigean spring tides.

There is, however, a cycle related to the perigee precession, which VL24 does not mention. The largest spring tides occur when perigee aligns with either spring or fall equinox (or summer or winter solstice, depending on the tidal regime), and this occurs at roughly half the 8.85-y period, giving rise to the well-known quasi-4.5 year cycle in tidal extremes (Woodworth & Blackman, 2004; Ray & Merrifield, 2019; Pugh & Woodworth, 2014, Fig. 3.16).

Perigee argument, period 6.00 y. There is little justification for this period. It is true that the mean longitude of the moon's perigee, moving relative to the equinox with period 8.85 y, also moves relative to the moving node with period 6.00 y, simply because $(1/8.85 + 1/18.6) = 1/6.00$ (the two frequencies are added, not subtracted, because the moon's node and perigee move in opposite directions). However, this is merely a relative motion that has no direct effect on the ocean. There is no tidal potential associated with this motion (Cartwright & Tayler, 1971), nor is any major tidal constituent modulated at this period. An indirect effect, from some hypothetical nonlinear combination of 18.6 and 8.85-y sinusoids, could potentially induce oscillations of 6 y, but certainly not if the 8.85-y sinusoids do not exist.

Keeling & Whorf (1997) argued that, over the period 1899–1947, extreme tides had induced a 6-y periodicity in global mean temperatures. As even they acknowledged, it seems implausible that oscillations in global temperature could be induced by isolated extreme tide events, spaced years apart, each event lasting only a few hours and each being barely larger than a typical perigean spring tide. Munk et al. (2002) discussed the wholly unlikely applicability of the idea. The implausibility only grew when it was discovered that the Keeling-Whorf catalog of extreme tides was inaccurate and that the true recurrence times of tidal extremes do not follow their reported patterns (Ray, 2007, Fig.5). The Keeling-Whorf study cannot salvage a 6-y period for ENSO cycle-fitting.

3.2. Interaction frequencies?

Given that two of VL24's three fundamental lunar frequencies are without significant influence on the ocean, all but one of the supposed interaction frequencies disappear. The one remaining is between the solar cycle (VL24 uses a period of 11.5 y) and the nodal precession, with interaction period of 30.1 y. VLP24 give three other possible periods for the solar cycle, which in turn give three other interaction periods of 21.6, 24.1, and 26.9 y. With so many free periods to choose from, and no evident physical relationships to ENSO, this supposed interaction between the nodal cycle and the solar cycle must be treated as merely conjectural.

VL24 also claims periods at 3 and 6 times the nodal precession period, or 56 and 112 years. As noted above, VLP24 take this further, imagining periods of 2, 3, 4, and 6 times the nodal period. There is no physical explanation for how such "subharmonics" could possibly arise, and we can think of none. It is similar to suggesting that the M_2 tide (period 12.4 h) is capable of generating sea-level oscillations of 37 h, 74 h, etc., and this simply does not happen.

Finally, VL24 also employs a second harmonic of the nodal precession at period 9.3 y. This harmonic is conceivable in a climate variable, and we can think of three possible mechanisms, although upon examination each seems unlikely: (1) A second harmonic is obviously possible if the nodal cycle in ocean mixing is not a pure sinusoid. The nodal modulation of diurnal (or semidiurnal) current velocities is mostly a pure sinusoid (see next point), but mixing depends on higher powers of velocity (Loder & Garrett, 1978), thus bringing in higher harmonics. The higher harmonics, however, must be smaller than the fundamental, which is already so small that it has been difficult to detect in climate. Thus, the 9.3-y effect, if it exists through this mechanism, is likely insignificant. (2) A 9.3-y period does arise as a second harmonic of the nodal modulation of major lunar tides. The largest is for O_1. That nodal line (Doodson number 145.535) is only 3% of the main O_1 nodal line and only 0.6% of the primary O_1 line (Cartwright & Tayler, 1971). Given that the main nodal modulation's impact on climate is already small and difficult to detect, this second harmonic must also be of little significance. (3) A final possibility is to note that 18.6-y modulations of diurnal and semidiurnal tides are mostly 180° out-of-phase (Loder & Garrett, 1978). Thus, a mechanism like ocean mixing that depends nonlinearly on current speed could generate a 9.3-y periodicity—strong diurnal tides followed 9.3 y later by strong semidiurnals—if the diurnal and semidiurnal tides at a given location are both large enough to significantly affect mixing (Ray, 2007). If this occurs it has not yet been observed, but it is a conceivable mechanism for 9.3-y variability.

4. Conclusion

There is no physical justification for any climate impact of the 13 astronomical frequencies used by VL24, aside from the solar cycle (not discussed here, but see Pittock (1978, 2009)), the lunar nodal period (e.g., Joshi et al., 2023), and (remotely possible) the nodal second harmonic. Two of the VL24 fundamental periods have no likely impact on climate whatsoever, and therefore most of the supposed interaction frequencies vanish. Moreover, the assignment of statistical significance to the cycle fitting in VL24 is inappropriate. A dozen or so selectively chosen (yet physically doubtful) frequencies can fit a random ENSO-like time series almost as easily as the real ENSO time series. Cycle-fitting of a random series can have no predictive ability, and we cannot expect it to have any for the real ENSO series either.

Data availability statement

The ENSO index nino3.4 is available from `https://www.esrl.noaa.gov/psd/data/climateindices/list/`.

Acknowledgments

For useful discussions we thank Brian Beckley, William Kessler, Gary Mitchum, Philip Woodworth, and Edward Zaron.

References

Ambaum, M. H. P. (2010). Significance tests in climate science. *J. Climate*, *23*, 5927–5932. doi: 10.1175/2010JCLI3746.1

Amdur, T., Stine, A. R., & Huybers, P. (2021). Global surface temperature response to 11-yr solar cycle forcing consistent with general circulation model results. *J. Climate*, *34*, 2893–2903. doi: 10.1175/JCLI-D-20-0312.1

Cartwright, D. E., & Tayler, R. J. (1971). New computations of the tide-generating potential. *Geophys. J. R. astr. Soc.*, *23*, 45–74.

Davison, A. C., & Hinkley, D. V. (1997). *Bootstrap methods and their application*. Cambridge: Cambridge Univ. Press.

Doodson, A. T. (1924). Perturbations of harmonic tidal constants. *Proc. Royal Soc.*, *106*(739), 513–526.

Feng, X., Tsimplis, M. N., & Woodworth, P. L. (2015). Nodal variations and long-term changes in the main tides on the coasts of China. *J. Geophys. Res.: Oceans*, *120*, 1215–1232. doi: 10.1002/2014JC010312

Godin, G. (1988). *Tides*. Ensenada Baja California, Mexico: CICESE.

Joshi, M., Hall, R. A., Stevens, D. P., & Hawkins, E. (2023). The modelled climatic response to the 18.6-year lunar nodal cycle and its role in decadal temperature trends. *Earth Syst. Dynam.*, *14*, 443–455. doi: 10.5194/esd-14-443-2023

Keeling, C. D., & Whorf, T. P. (1997). Possible forcing of global temperature by the oceanic tides. *Proc. Nat. Acad. Sci.*, *94*, 8321–8328.

Loder, J. W., & Garrett, C. (1978). The 18.6-year cycle of sea surface temperature in shallow seas due to variations in tidal mixing. *J. Geophys. Res.*, *83*, 1967–1970.

Munk, W. H., Dzieciuch, M., & Jayne, S. (2002). Millennial climate variability: Is there a tidal connection? *J. Climate*, *15*, 370–385.

Osafune, S., Kouketsu, S., Masuda, S., & Sugiura, N. (2020). Dynamical ocean response controlling the eastward movement of a heat content anomaly caused by the 18.6-year modulation of localized tidally induced mixing. *J. Geophys. Res.: Oceans*, *125*, e2019JC015513. doi: 10.1029/2019JC015513

Osafune, S., & Yasuda, I. (2013). Remote impacts of the 18.6 year period modulation of localized tidal mixing in the North Pacific. *J. Geophys. Res.*, *118*, 3128–3137. doi: 10.1002/jgrc.20230

Percival, D. B., & Walden, A. T. (1993). *Spectral analysis for physical applications*. Cambridge: Cambridge Univ. Press.

Pittock, A. B. (1978). A critical look at long-term sun-weather relationships. *Rev. Geophys. Space Phys.*, *16*, 400–420.

Pittock, A. B. (2009). Can solar variations explain variations in the earth's climate? *Clim. Change*, *96*, 483–487. doi: 10.1007/s10584-009-9645-8

Pugh, D. T., & Woodworth, P. L. (2014). *Sea level science: Understanding tides, surges, tsunamis and mean sea-level changes*. Cambridge: Cambridge Univ. Press.

Ray, R. D. (2007). Decadal climate variability: Is there a tidal connection? *J. Climate*, *20*, 3542–3560. doi: 10.1175/JCLI4193.1

Ray, R. D., & Merrifield, M. A. (2019). The semiannual and 4.4-year modulations of extreme high tides. *J. Geophys. Res.: Oceans*, *124*, 5907–5922. doi: 10.1029/2019JC015061

Ray, R. D., & Talke, S. A. (2019). Nineteenth-century tides in the Gulf of Maine and implications for secular trends. *J. Geophys. Res.: Oceans*, *124*, 7046–7067. doi: 10.1029/2019JC015277

Timmer, J., & König, M. (1995). On generating power law noise. *Astro. Astrophys.*, *300*, 707–710.

Valle-Levinson, A. (2024). Linkage of El-Niño-Southern Oscillation to astronomic forcing. *Environ. Res. Lett.*, *19*, 104004. doi: 10.1088/1748-9326/ad7046

Valle-Levinson, A., Marani, M., Carniello, L., D'Alpaos, A., & Lanzoni, S. (2021). Astronomic link to anomalously high mean sea level in the northern Adriatic Sea. *Estuar. Coastal Shelf Sci.*, *257*, 107418. doi: 10.1016/j.ecss.2021.107418

Valle-Levinson, A., & Pattiaratchi, C. (2024). Filling in Munk's 'orbital gap' in climate and sea-level variability. *Environ. Res. Lett.*, *19*, 114030. doi: 10.1088/1748-9326/ad7ee5

Woodworth, P. L., & Blackman, D. L. (2004). Evidence for systematic changes in extreme high waters since the mid-1970s. *J. Climate*, *17*(6), 1190–1197.